



## Experiment Report Form

**The double page inside this form is to be filled in by all users or groups of users who have had access to beam time for measurements at the ESRF.**

Once completed, the report should be submitted electronically to the User Office via the User Portal:

<https://www.esrf.fr/misapps/SMISWebClient/protected/welcome.do>

### ***Reports supporting requests for additional beam time***

Reports can be submitted independently of new proposals – it is necessary simply to indicate the number of the report(s) supporting a new proposal on the proposal form.

The Review Committees reserve the right to reject new proposals from groups who have not reported on the use of beam time allocated previously.

### ***Reports on experiments relating to long term projects***

Proposers awarded beam time for a long term project are required to submit an interim report at the end of each year, irrespective of the number of shifts of beam time they have used.

### ***Published papers***

All users must give proper credit to ESRF staff members and proper mention to ESRF facilities which were essential for the results described in any ensuing publication. Further, they are obliged to send to the Joint ESRF/ ILL library the complete reference and the abstract of all papers appearing in print, and resulting from the use of the ESRF.

Should you wish to make more general comments on the experiment, please note them on the User Evaluation Form, and send both the Report and the Evaluation Form to the User Office.

### **Deadlines for submission of Experimental Reports**

- 1st March for experiments carried out up until June of the previous year;
- 1st September for experiments carried out up until January of the same year.

### **Instructions for preparing your Report**

- fill in a separate form for each project or series of measurements.
- type your report, in English.
- include the reference number of the proposal to which the report refers.
- make sure that the text, tables and figures fit into the space available.
- if your work is published or is in press, you may prefer to paste in the abstract, and add full reference details. If the abstract is in a language other than English, please include an English translation.



	<b>Experiment title:</b> Monoclinic distortions and orbital-ordering in the Ca-doped Mott insulator $\text{Pr}_{1-x}\text{Ca}_x\text{VO}_3$	<b>Experiment number:</b> HS-4297
<b>Beamline:</b>	<b>Date of experiment:</b> from: 05/05/2011 to: 09/05/2011	<b>Date of report:</b> 27/05/2011
<b>Shifts:</b>	<b>Local contact(s):</b> P. M. Abdala	<i>Received at ESRF:</i>
<b>Names and affiliations of applicants (* indicates experimentalists):</b> <b>M. Reehuis *</b> ,Helmholtz-Zentrum für Materialien und Energie, D-14109 Berlin, Germany C. Ulrich, University of New South Wales, Sydney, New South Wales 2052, Australia B. Keimer, Max-Planck-Institut für Festkörperforschung, D-70569 Stuttgart, Germany J. Fujioka, Department of Applied Physics, University of Tokyo, 113 Tokyo, Japan S. Miyasaka, Department of Physics, Osaka University, Osaka 560-0043, Japan Y. Tokura, Department of Applied Physics, University of Tokyo, 113 Tokyo, Japan <b>P. Pattison, SNBL at ESRF, F-38042 Grenoble Cedex 9, France</b>		

### Report:

Ternary transition-metal oxides with perovskite structure have attracted considerable attention due to their unusual phase behavior and physical properties, which are consequences of an intricate interplay between charge, orbital, and spin ordering. Orthovanadates of chemical composition  $R\text{VO}_3$ , with  $R = \text{Y}$  or a trivalent rare-earth metal atom, are particularly interesting examples, as they undergo multiple orbital and magnetic ordering transitions as a function of temperature [1-6]. At room temperature these materials exhibit the orthorhombic  $\text{GdFeO}_3$ -type structure with space group  $Pbnm$ . With decreasing temperature, they undergo a structural phase transition ( $T_S$ ), ascribed to orbital ordering, into a phase described by the monoclinic space group  $P2_1/b$ , and a Néel transition ( $T_N$ ) associated with the formation of a  $C$ -type magnetic structure of the spin-1 moments of  $\text{V}^{3+}$ . For  $\text{PrVO}_3$  these transitions set in at  $T_S = 171$  K and  $T_N = 140$  K, respectively. Recently the electronic phase diagram has been investigated for the Ca-doped vanadates  $\text{Pr}_{1-x}\text{Ca}_x\text{VO}_3$  [4]. The increase of the doping level  $x(\text{Ca})$  causes a melting of the orbital and spin order followed by a metal-insulator transition at  $x(\text{Ca}) = 0.23$ .

In order to investigate in detail the orthorhombic and monoclinic structure of Ca-doped vanadates  $\text{Pr}_{1-x}\text{Ca}_x\text{VO}_3$  we performed high-resolution powder diffraction studies at the ESRF in Grenoble. For the experiment we took single crystal samples, and ground fragments to fine powders, which were mounted in a glass capillary of diameter 0.5 mm. Complete powder patterns on the BM1B (Swiss-Norwegian) beam line with a  $2\theta$ -range between 1 and  $55^\circ$  were collected using the wavelength  $\lambda = 0.50214(4)$  Å. Rietveld refinements of the powder diffraction data were carried out with the program *FullProf* using the atomic scattering factors

provided by the program [7]. Refinements of the diffraction patterns  $\text{PrVO}_3$ ,  $\text{Pr}_{0.90}\text{Ca}_{0.10}\text{VO}_3$  and  $\text{Pr}_{0.80}\text{Ca}_{0.20}\text{VO}_3$  collected at 15 K were performed in the monoclinic space group  $P2_1/b$ . For comparison we collected a data set of the orthorhombic phase (space group  $Pbnm$ ) of  $\text{Pr}_{0.90}\text{Ca}_{0.10}\text{VO}_3$  at 290 K. Here the V- and O2-atoms are located in the Wyckoff positions  $4b(\frac{1}{2},0,0)$  and  $8d(x,y,z)$ , respectively, while the O1- and Pr(Ca)-atoms are located at the position  $4c(x,y,\frac{1}{4})$ . In the monoclinic phase the vanadium atoms are located in the positions  $2c(\frac{1}{2},0,0)$  and  $2d(\frac{1}{2},0,\frac{1}{2})$ , while the Pr(Ca)- and the three different O-atoms (O1, O2 and O3) are located in the position  $4e(x,y,z)$ . During the refinements a total of 12 and 7 positional parameters were allowed to vary in the space groups  $P2_1/b$  and  $Pbnm$ , respectively. The crystal structure refinements of the three compounds  $\text{PrVO}_3$ ,  $\text{Pr}_{0.90}\text{Ca}_{0.10}\text{VO}_3$  and  $\text{Pr}_{0.80}\text{Ca}_{0.20}\text{VO}_3$  resulted in very satisfactory  $R_F$ -values between 0.015 and 0.023. The refined positional parameters finally allowed us to determine precisely the interatomic distances. The bond distances between the V- and O-atoms in the  $\text{VO}_6$ -octahedra as well as the lattice parameters are presented in Fig. 1.

The onset of orbital ordering appears at the structural phase transition temperature  $T_S$ , while the C-type spin ordering of the V-sublattice sets in at the lower lying Néel temperature  $T_N$ . The increase of the doping level  $x(\text{Ca})$  causes a decrease of the transition temperatures  $T_S$  and  $T_N$  as well as the lattice parameters  $a$  and  $b$ , while the  $c$ -axis remains almost unchanged (Fig. 1). In the range  $0 \leq x(\text{Ca}) \leq 0.20$  the cell volume shows a relatively strong decrease of 1.93%. The change of V-O-bond distances in the two different  $\text{VO}_6$ -octahedra (of V1 and V2) is shown in the lower part of the diagram of Fig. 1. Up to a doping level of  $x(\text{Ca}) = 0.20$  the V1-O22- and V2-O32-bonds are strongly elongated indicating the presence of the *Jahn-Teller* effect (Fig. 1). Interestingly the *Jahn-Teller* effect is still established at the doping level  $x(\text{Ca}) = 0.20$ . This is close to the critical level  $x(\text{Ca}) = 0.23$ , where the metal-insulator transition was found [4]. The change of the apical bond lengths  $d(\text{V1-O1})$  and  $d(\text{V2-O1})$  is quite unusual. In  $\text{PrVO}_3$  these bond lengths [ $d(\text{V1-O1}) = 1.981(8) \text{ \AA}$ ,  $d(\text{V2-O1}) = 1.985(8) \text{ \AA}$ ] are very similar. But with increasing  $x(\text{Ca})$  these bond lengths differ significantly. For  $\text{Pr}_{0.80}\text{Ca}_{0.20}\text{VO}_3$  finally the values  $d(\text{V1-O1}) = 2.008(11) \text{ \AA}$  and  $d(\text{V2-O1}) = 1.937(11) \text{ \AA}$  have been obtained.

The  $\text{Ca}^{2+}$  and  $\text{Pr}^{3+}$  ions are surrounded by 8  $\text{O}^{2-}$ -ions in a distorted cubic coordination. All the 8 bond distances in  $\text{PrVO}_3$  show different values between 2.367(3) and 2.713(6)  $\text{ \AA}$ . A very similar range between 2.363(3) and 2.708(8)  $\text{ \AA}$  could be observed for the Ca-doped vanadate  $\text{Pr}_{0.80}\text{Ca}_{0.20}\text{VO}_3$ . For both compounds the averaged  $d$ -values  $d_{\text{av}} = 2.534(5) \text{ \AA}$  ( $\text{PrVO}_3$ ) and  $d_{\text{av}} = 2.535(7) \text{ \AA}$  ( $\text{Pr}_{0.80}\text{Ca}_{0.20}\text{VO}_3$ ) are practically the same. This can be ascribed to the fact that the ionic radii of both ions  $\text{Ca}^{2+}$  ( $r = 1.12 \text{ \AA}$ ) and  $\text{Pr}^{3+}$  ( $r = 1.126 \text{ \AA}$ ) are very similar [8]. On the other hand an increase of the Ca-doping level [ $0 \leq x(\text{Ca}) \leq 1$ ] changes the charge of the vanadium ions from 3+ to 4+ assuming a pure ionic system. Accordingly one expects for  $\text{Pr}_{0.90}\text{Ca}_{0.10}\text{VO}_3$  and  $\text{Pr}_{0.80}\text{Ca}_{0.20}\text{VO}_3$  a mixed valency with charges of +2.9 and +2.8, respectively. Due to the different ionic radii  $r(\text{V}^{3+}) = 0.640 \text{ \AA}$  and  $r(\text{V}^{4+}) = 0.58 \text{ \AA}$  (in an octahedral coordination) [8] the averaged  $d$ -value (from the three different bond distances in the  $\text{VO}_6$ -octahedra) decreases with increasing Ca-doping level. In fact, we observed a slight decrease of the averaged  $d$ -value:  $d_{\text{av}} = 2.005(7) \text{ \AA}$  ( $\text{PrVO}_3$ )  $>$   $d_{\text{av}} = 1.994(8) \text{ \AA}$  ( $\text{Pr}_{0.90}\text{Ca}_{0.10}\text{VO}_3$ )  $>$   $d_{\text{av}} = 1.985(9) \text{ \AA}$  ( $\text{Pr}_{0.80}\text{Ca}_{0.20}\text{VO}_3$ ). At 290 K we obtained for  $\text{Pr}_{0.90}\text{Ca}_{0.10}\text{VO}_3$  the value  $d_{\text{av}} = 1.9935(14)$ . Despite to the fact that the *Jahn-Teller* effect is only active in the monoclinic phase the  $d_{\text{av}}$ -values are almost unchanged.

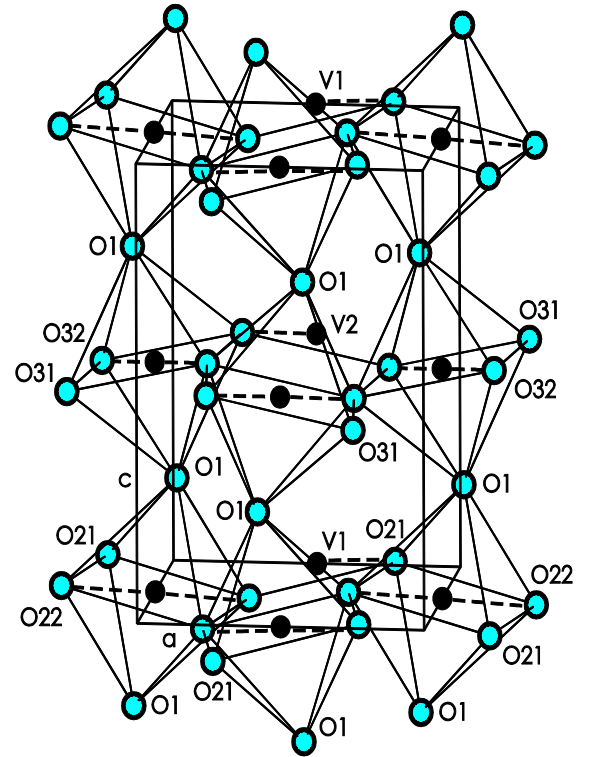
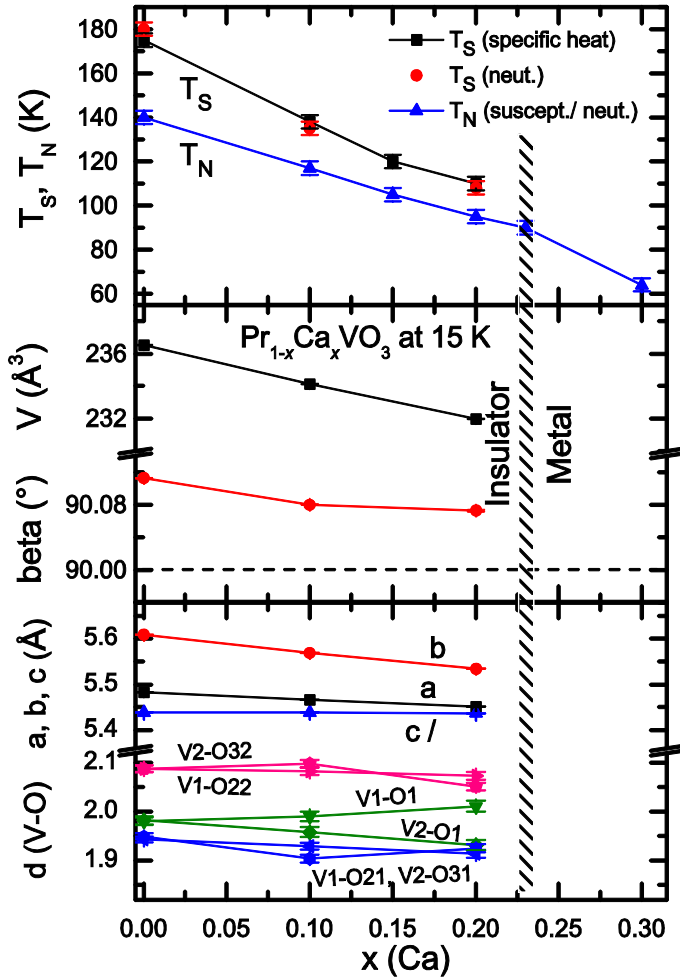


**Fig. 1.** Change of structural and magnetic properties in the system  $\text{Pr}_{1-x}\text{Ca}_x\text{VO}_3$  as a function of the doping level  $x(\text{Ca})$ . In the insulating state the V1-O22- and V2-O32-bonds are strongly elongated due to the presence of the *Jahn-Teller* effect. The network of distorted corner-shared  $\text{VO}_6$ -octahedra in the monoclinic phase of  $\text{Pr}_{1-x}\text{Ca}_x\text{VO}_3$  is also shown. The dashed lines represent the elongated V-O-bonds due to the *Jahn-Teller* effect.

## References

1. G. R. Blake, T. T. M. Palstra, Y. Ren, A. A. Nugroho, A. A. Menovsky, Phys. Rev. Lett. **87**, 245501 (2001); Phys. Rev. B **65** (2002) 174112.
2. S. Miyasaka, Y. Okimoto, M. Iwama, and Y. Tokura, Phys. Rev. B **68** (2003) 100406(R).
3. C. Ulrich, G. Khaliullin, J. Sirker, M. Reehuis, M. Ohl, S. Miyasaka, Y. Tokura, B. Keimer, Phys. Rev. Lett. **91** (2003) 257202.
4. J. Fujijoka, S. Miyasaka, Y. Tokura, Phys. Rev. B **72** (2005) 024460.
5. M. Reehuis, C. Ulrich, P. Pattison, B. Ouladdiaf, M. C. Rheinstädter, M. Ohl, L. P. Regnault, S. Miyasaka, Y. Tokura, B. Keimer, Phys. Rev. B **73** (2006) 094440.
6. M. Reehuis, C. Ulrich, P. Pattison, S. Miyasaka, Y. Tokura, B. Keimer, Phys. Rev. B **73** (2006) 094440.
7. J. Rodriguez-Carvajal, Physica B **192**, 55 (1993).
8. R. D. Shannon, Acta Cryst. A **32** (1976) 751.